

Electronic Supplementary Information

A standard for normalizing the outputs of triboelectric nanogenerators in various modes

**Da Zhao,^{‡ab} Xin Yu,^{‡a} Jianlong Wang,^{‡ab} Qi Gao,^a Zhenjie Wang,^a
Tinghai Cheng^{*ab} and Zhong Lin Wang^{*ac}**

^a *Beijing Institute of Nanoenergy and Nanosystems, Chinese Academy of Sciences, Beijing 101400, P. R. China. E-mail: chengtinghai@binn.cas.cn.*

^b *School of Mechatronic Engineering, Changchun University of Technology, Changchun, Jilin 130012, P. R. China.*

^c *School of Materials Science and Engineering, Georgia Institute of Technology, Atlanta, GA 30332-0245, USA. E-mail: zhong.wang@mse.gatech.edu.*

† Electronic Supplementary Information (ESI) available. See DOI:
10.1039/x0xx00000x

‡ *These authors contributed equally to this work.*

Supplementary Figures

Fig. S1. Schematic diagram of four different mode TENGs.

Fig. S2. Normalized analysis of output voltage and current for mechanical structures of C-S and L-S mode TENGs.

Fig. S3. Normalized analysis of output voltage and current for mechanical structures of S-E and F-S mode TENGs.

Fig. S4. Normalized analysis of output performance under different resistances and capacitances for contact area and film thickness in S-E and F-S mode TENGs.

Fig. S5. Normalized analysis of output voltage and current for external excitations of C-S and L-S mode TENGs.

Fig. S6. Normalized analysis of output voltage and current for external excitations of S-E and F-S mode TENGs.

Fig. S7. Normalized analysis of output performance under different resistances and capacitances for displacement distance and applied force in S-E and F-S mode TENGs.

Fig. S8. Normalized analysis of output voltage and current for triggering frequency of C-S and L-S mode TENGs.

Fig. S9. Normalized analysis of output voltage and current for triggering frequency of S-E and F-S mode TENGs.

Fig. S10. Normalizing outputs under different resistances and capacitances for triggering frequency in S-E and F-S mode TENGs.

Fig. S11. Normalization of optimal peak power for TENGs of S-E mode and F-S mode under different load resistance and capacitance.

Fig. S12. Photograph of the evaluating prototype.

Fig. S13. Photograph of a variable frequency prototype.

Supplementary Tables

Table S1. The influence degree of each factor for TENGs

Table S2. The parameters list of the evaluated prototype.

Table S3. The matching resistance and capacitance of the evaluated prototypes.

Supplementary Notes

Supplementary Note 1. Theoretical calculation.

Supplementary Note 2. Calculation of matching reactance for evaluation prototypes.

Supplementary Figures

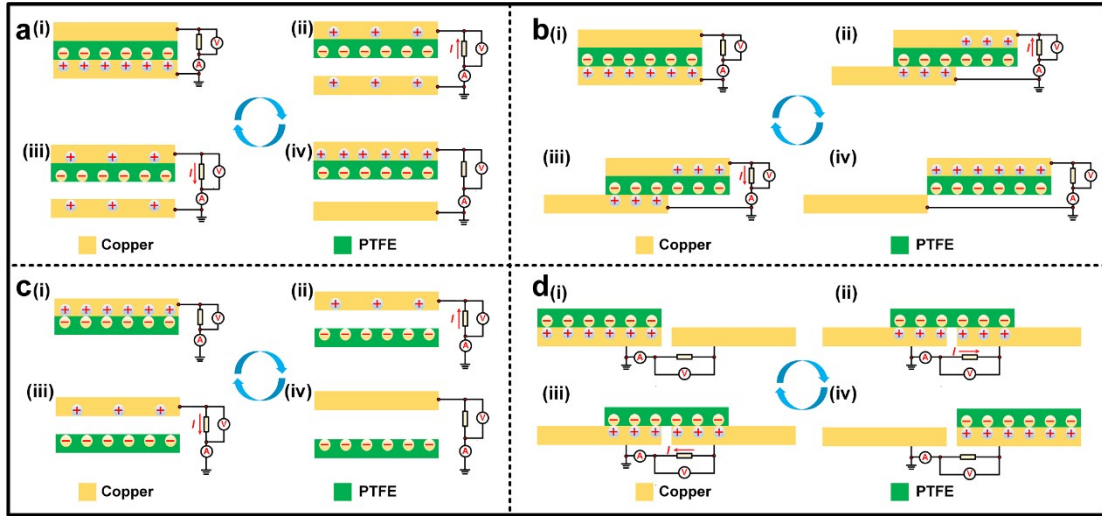


Fig. S1. Schematic diagram of four different mode TENGs. (a) C-S mode TENG, (b) L-S mode TENG, (c) S-E mode TENG, (d) F-S mode TENG.

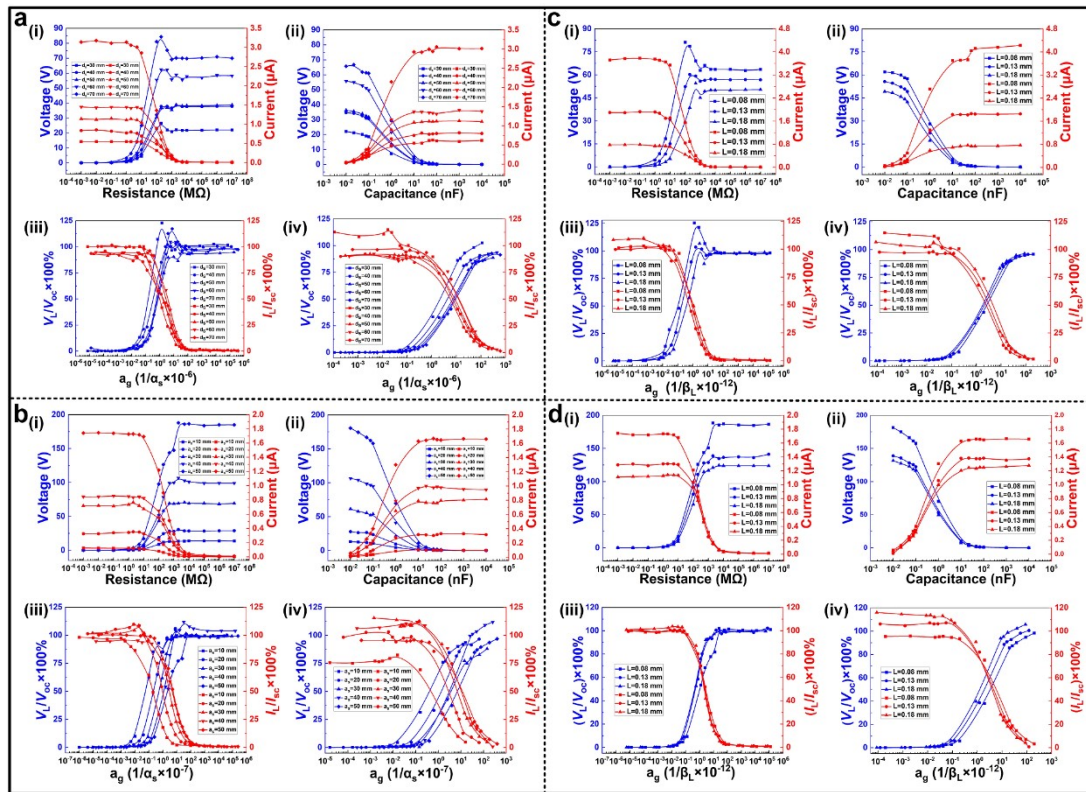


Fig. S2. Normalized analysis of output voltage and current for mechanical structures of C-S and L-S mode TENGs. The output performance (i, ii) and normalized data (iii, iv) of C-S and L-S (b, d) mode TENGs in different contact areas (a, b) and film thicknesses (c, d).

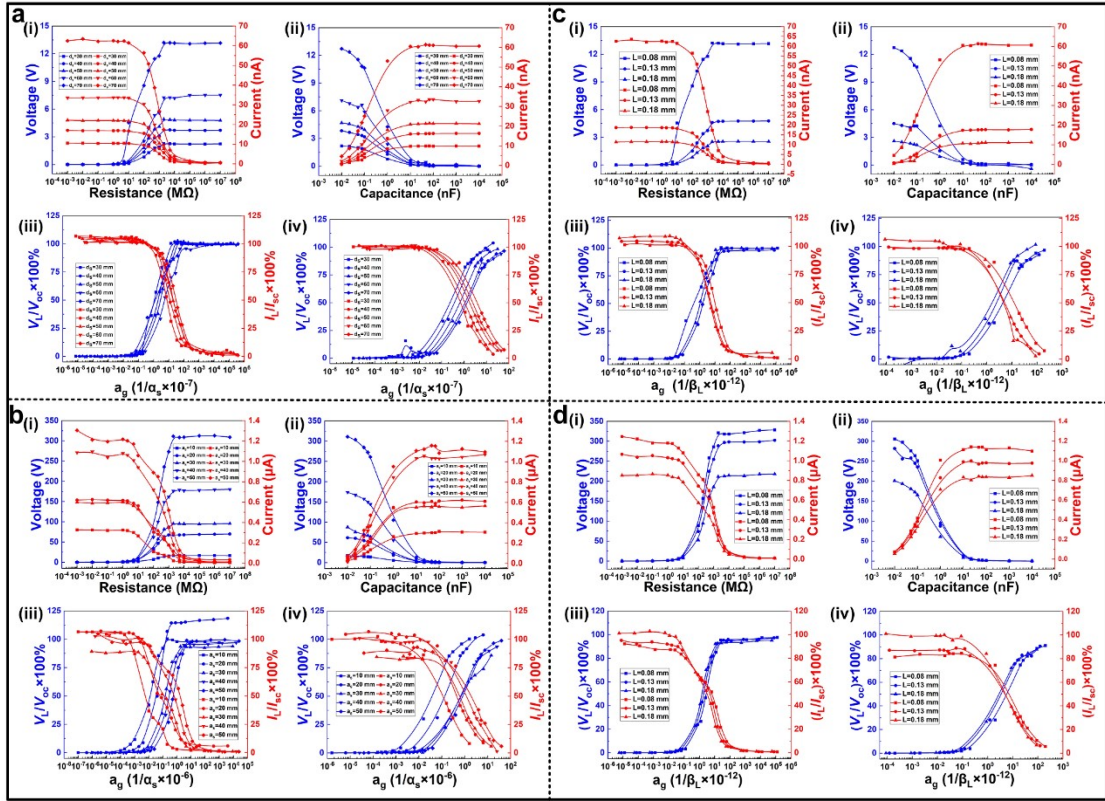


Fig. S3. Normalized analysis of output voltage and current for mechanical structures of S-E and F-S mode TENGs. The output performance (i, ii) and normalized data (iii, iv) of S-E (a, c) and F-S (b, d) mode TENGs in different contact areas (a, b) and film thicknesses (c, d).

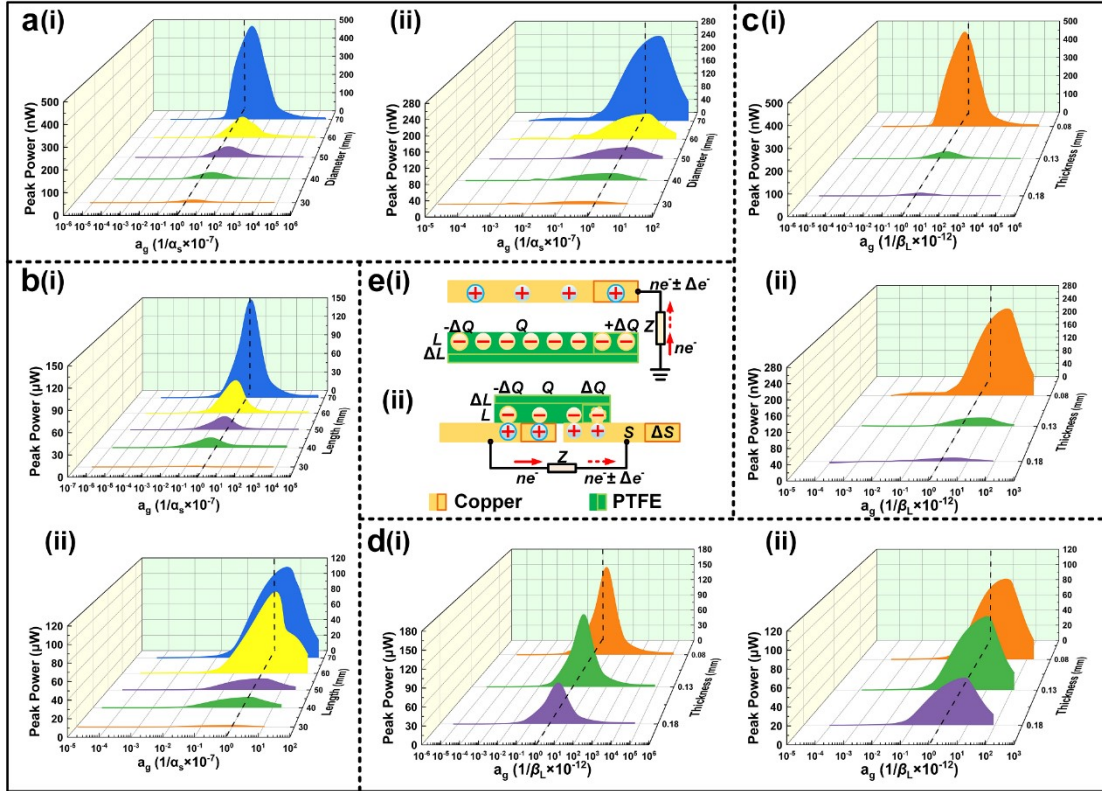


Fig. S4. Normalized analysis of output performance under different resistances (i) and capacitances (ii) for contact area (a, b) and film thickness (c, d) in S-E (a, c) and F-S (b, d) mode TENGs. (e) Diagram of charge transfer in S-E and F-S mode TENGs with changes in contact area and film thickness.

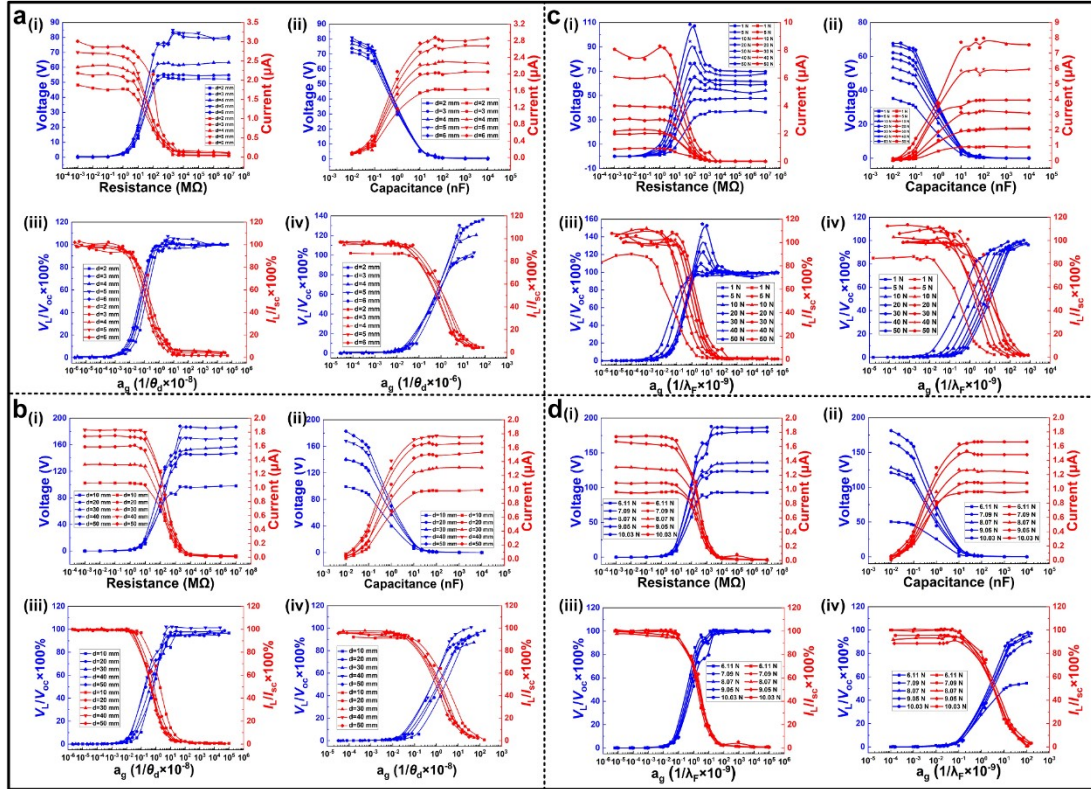


Fig. S5. Normalized analysis of output voltage and current for external excitations of C-S and L-S mode TENGs. The output performance (i, ii) and normalized data (iii, iv) of C-S (a, c) and L-S (b, d) mode TENGs in different displacement distances (a, b) and applied forces (c, d).

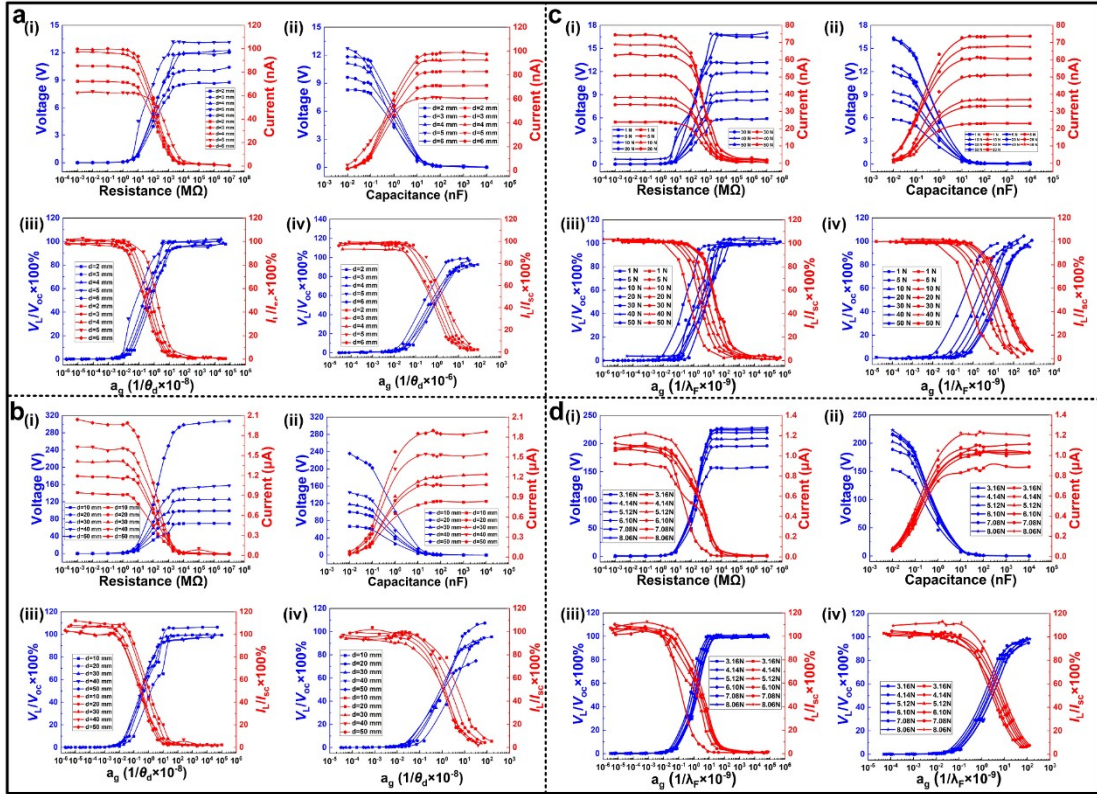


Fig. S6. Normalized analysis of output voltage and current for external excitations of S-E and F-S mode TENGs. The output performance (i, ii) and normalized data (iii, iv) of S-E (a, c) and F-S (b, d) mode TENGs in different displacement distances (a, b) and applied forces (c, d).

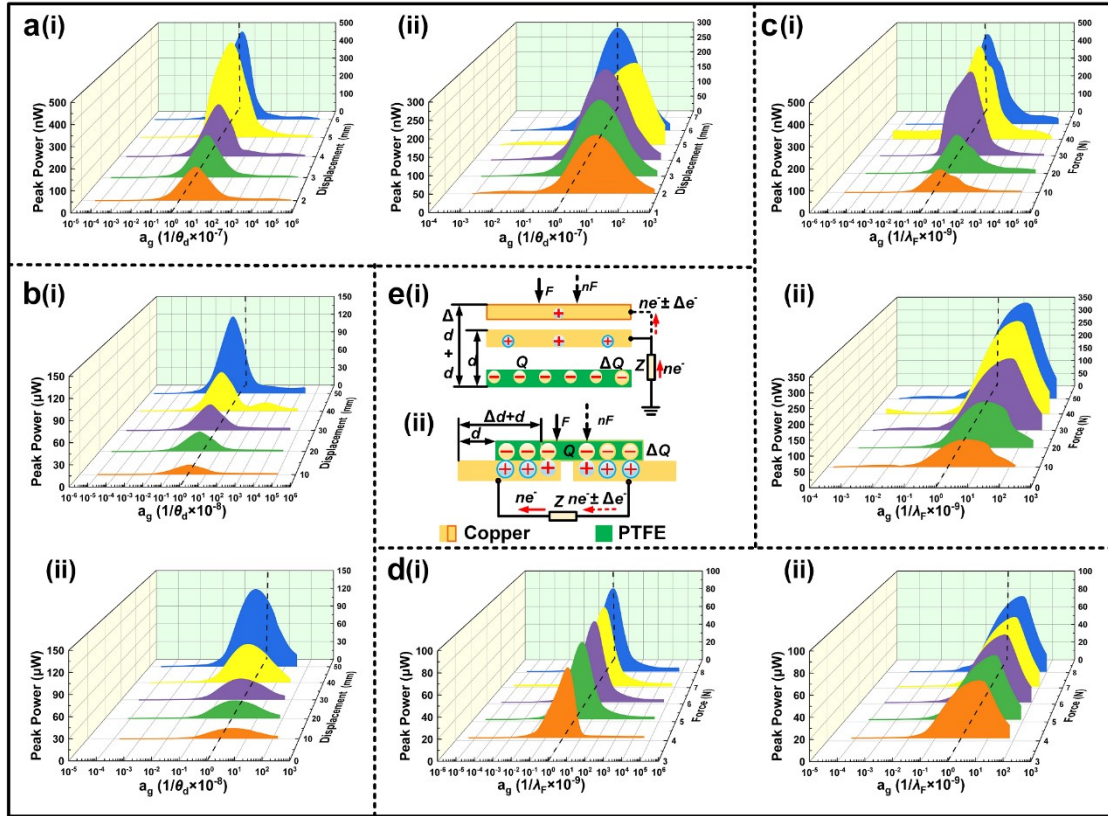


Fig. S7. Normalized analysis of output performance under different resistances (i) and capacitances (ii) for displacement distance (a, b) and applied force (c, d) in S-E (a, c) and F-S (b, d) mode TENGs. (e) Diagram of charge transfer in S-E and F-S mode TENGs with changes in displacement distance and applied force.

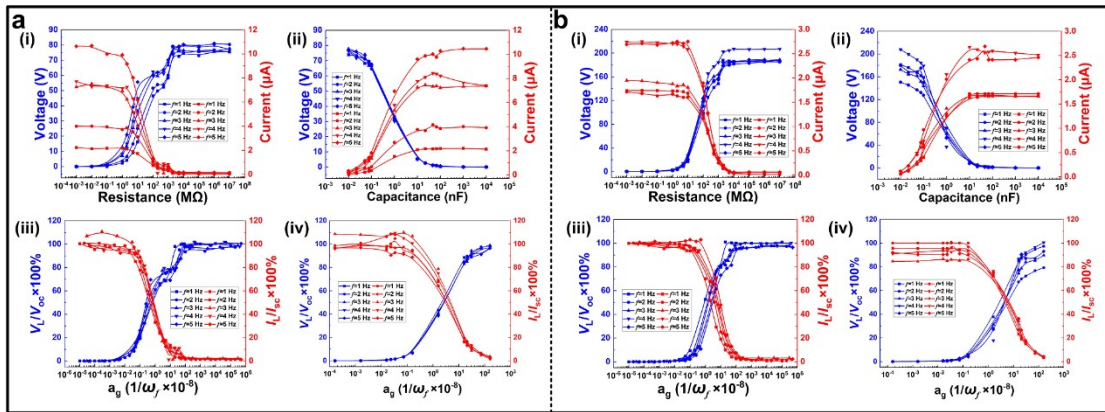


Fig. S8. Normalized analysis of output voltage and current for triggering frequency of C-S and L-S mode TENGs. The output performance (i, ii) and normalized data (iii, iv) of C-S (a) and L-S (b) mode TENGs in different frequencies.

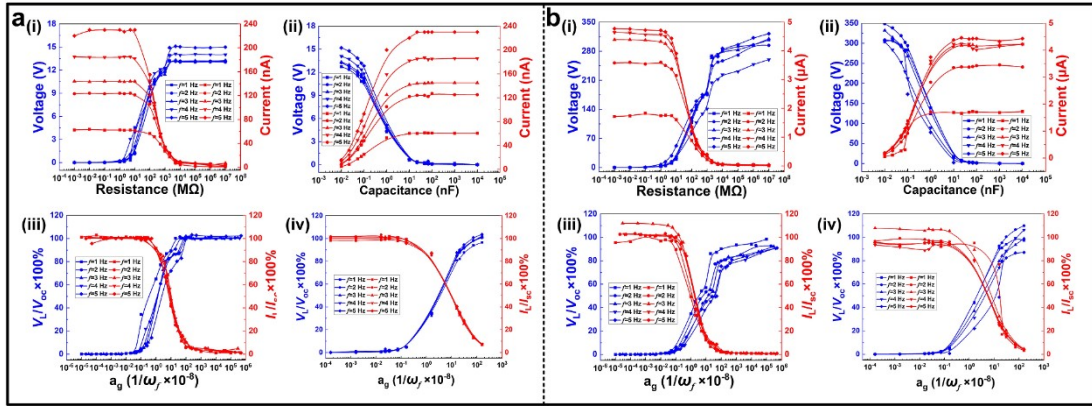


Fig. S9. Normalized analysis of output voltage and current for triggering frequency of S-E and F-S mode TENGs. The output performance (i, ii) and normalized data (iii, iv) of S-E (a) and F-S (b) mode TENGs in different frequencies.

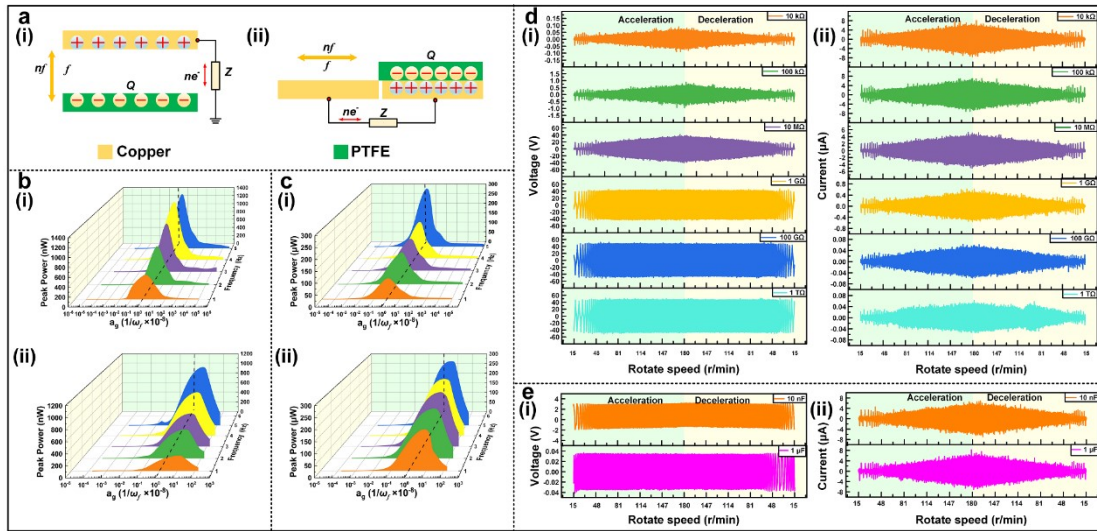


Fig. S10. Normalizing outputs under different resistances (i) and capacitances (ii) for triggering frequency in S-E (b) and F-S (c) mode TENGs. (a) Schematic diagram of S-E (i) and F-S (ii) mode TENGs changing with triggering frequency. (d, e) The output performance of TENGs as triggering frequency changes under different resistances (d) and capacitances (e).

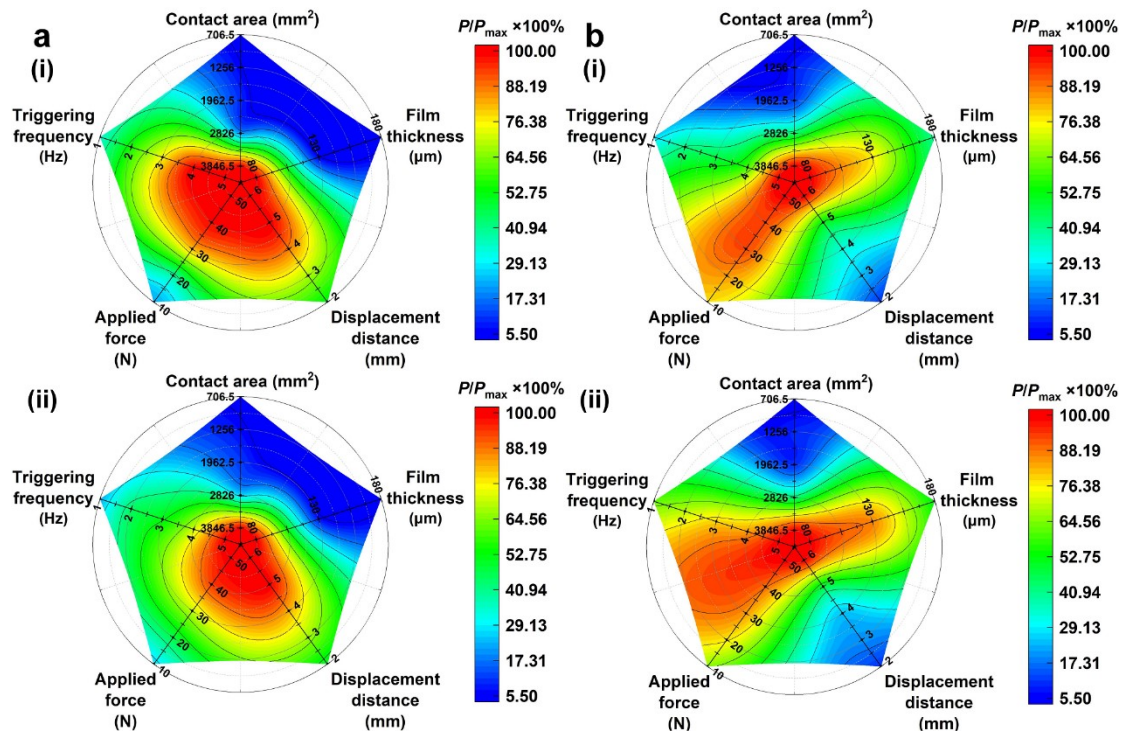


Fig. S11. Normalization of optimal peak power for TENGs of S-E mode (a) and F-S mode (b) under different load resistance (i) and capacitance (ii).

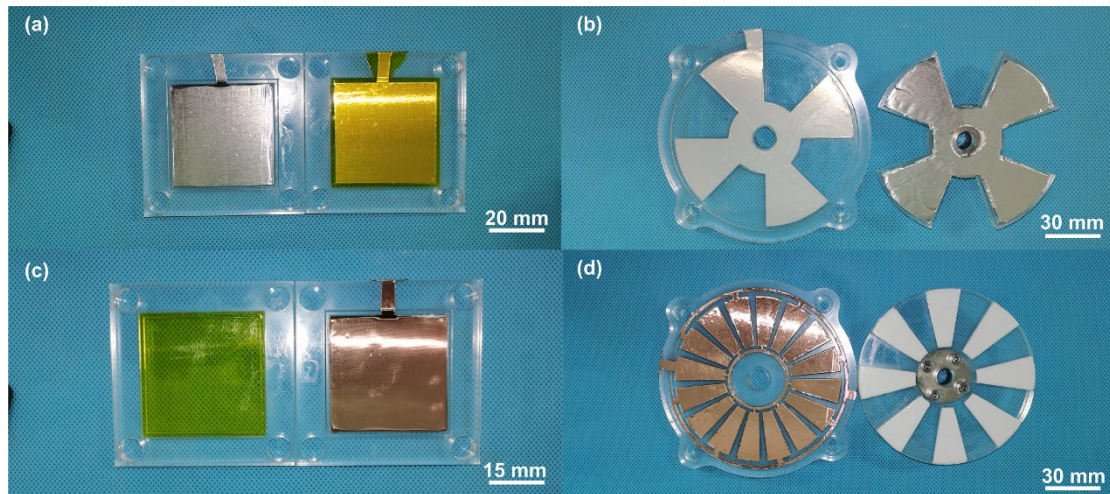


Fig. S12. Photograph of the evaluating prototype.

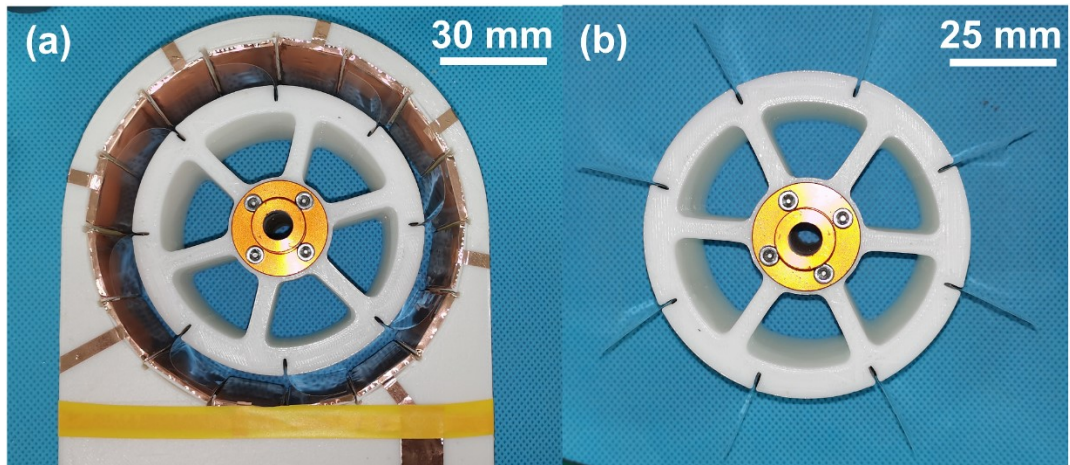


Fig. S13. Photograph of a variable frequency prototype.

Supplementary Tables

Table S1. The definitions of important parameters of the TENG.

Symbo	Definitions	Symbol	Definitions
I			
S	contact area	$C0$	internal capacitance
L	film thickness	CL	load capacitance
d	displacement distance	P_R	power of the load resistance
F	applied force	PC	power of the load capacitance
f	triggering frequency	σ	charge density
C_1	variable capacitance	t	time of current changes
C_2	constant capacitance	ρ	resistivity of the dielectric layer
R_0	internal resistance	k	the electrostatic force constant
C_3	inductive capacitors	$\epsilon r1$	the relative dielectric constant of dielectric layer
T	the thickness of triboelectric layer	$\epsilon r2$	the relative dielectric constant of environment.
$I1$	the load current	ag	reactance matching value
RL	matching resistance	a	the side length for L-S, F-S mode
CL	matching capacitor	I_0	internal current

Table S2. The influence degree of each factor for TENGs

Types	C-S mode		L-S mode		S-E mode		F-S mode		
	Load	R	C	R	C	R	C	R	C
Contact area		93.38	94.40	99.39	99.57	97.61	97.19	99.31	98.52
Film thickness		89.12	86.64	38.98	46.06	97.58	96.79	60.52	47.99
Displacement distance		58.94	48.97	61.96	70.03	47.84	50.47	88.66	89.22
Applied force		88.58	73.49	69.29	77.94	78.00	73.62	21.81	34.42
Triggering frequency		90.08	76.71	56.07	46.75	77.63	66.31	73.36	37.90

Table S3. The parameters list of the evaluated prototype.

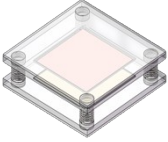

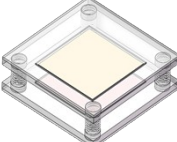

Working mode of TENGs	C-S mode	L-S mode	S-E mode	F-S mode
Electrode	Kapton+Al	PTFE+Al	Kapton+Cu	PTFE+Al
Contact area S (m²)	0.0025	0.0045	0.0025	0.0051
Film thickness L (mm)	0.05	0.18	0.05	0.08
Displacement distance d	5 mm	40°	5 mm	17.5°
Applied force F (N)	20 N	NA	20 N	NA
Triggering frequency f	1 Hz	30 r/min (2 Hz)	1 Hz	15 r/min (2 Hz)
Prototype				

Table S4. The matching resistance and capacitance of the evaluated prototypes.

	C-S mode	L-S mode	S-E mode	F-S mode
Resistance (R_0)	$10^{7\sim 8} \Omega$	$10^8 \Omega$	$10^{7\sim 8} \Omega$	$10^8 \Omega$
Capacitance (C_T)	10^{-9} F	$10^{-10\sim -9} \text{ F}$	$10^{-10\sim -9} \text{ F}$	$10^{-10\sim -9} \text{ F}$

Supplementary Notes

Supplementary Note 1. Theoretical calculation.

Eqs. (S1) and (S2) are the transformational power equations of the triboelectric nanogenerators (TENG).

$$P_R = \frac{I_0^2 R_0^2 R_L}{R_L^2 + \left(\frac{1}{2\pi f} \left(\frac{1}{C_1} + \frac{1}{C_2} \right) \right)^2} \quad (\text{S1})$$

$$P_C = \frac{I_0^2 R_0^2 \left(\frac{1}{2\pi f C_L} \right)}{\left(\frac{1}{2\pi f} \left(\frac{1}{C_1} + \frac{1}{C_2} + \frac{1}{C_L} \right) \right)^2} \quad (\text{S2})$$

The matching values for the contact area, film thickness, displacement distance, applied force and triggering frequency are shown in Eqs. (S4), (S6), (S9), (S11) and (S13), respectively.

$$\alpha_s = \sqrt{(\rho \cdot T)^2 + \left(\frac{2k}{f} \left(\frac{L}{\varepsilon_{r1}} + \frac{D}{\varepsilon_{r2}} \right) \right)^2} \quad (\text{S3})$$

$$\begin{cases} a_g = \frac{1}{\alpha_s} \mathfrak{g}(\Delta R_L \mathfrak{g} \Delta S) \\ a_g = \frac{1}{2\pi f} \mathfrak{g} \frac{1}{\alpha_s} \mathfrak{g} \left(\frac{\Delta S}{\Delta C_L} \right) \end{cases} \quad (\text{S4})$$

$$\beta_L \approx \frac{2k}{fS\varepsilon_{r1}} \quad (\text{S5})$$

$$\begin{cases} a_g \approx \frac{1}{\beta_L} \mathfrak{g} \frac{\Delta R_L}{\Delta L} \\ a_g \approx \frac{1}{2\pi f \beta_L} \mathfrak{g} \frac{1}{\Delta C_L \Delta L} \end{cases} \quad (\text{S6})$$

$$\theta_{d1} \approx \frac{2k}{fS\varepsilon_{r1}} \quad (\text{S7})$$

$$\theta_{d2} \approx \frac{2kL}{fa\varepsilon_{r1}} \quad (\text{S8})$$

$$\left\{ \begin{array}{l} a_g \approx \frac{1}{\theta_{d1}} \mathbf{g} \frac{\Delta R_L}{\Delta d} \text{ (C-S \& S-E modes)} \\ a_g \approx \frac{1}{\theta_{d1}} \mathbf{g} \Delta R_L \Delta d \text{ (L-S \& F-S modes)} \\ a_g \approx \frac{1}{2\pi f} \mathbf{g} \frac{1}{\theta_{d2}} \mathbf{g} \frac{1}{\Delta d \Delta C_L} \text{ (C-S \& S-E modes)} \\ a_g \approx \frac{1}{2\pi f} \mathbf{g} \frac{1}{\theta_{d2}} \mathbf{g} \frac{\Delta d}{\Delta C_L} \text{ (L-S \& F-S modes)} \end{array} \right. \quad (\text{S9})$$

$$\lambda_F \approx \frac{2k}{f \epsilon_{r1}} \quad (\text{S10})$$

$$\left\{ \begin{array}{l} a_g \approx \frac{1}{\lambda_F} \mathbf{g} \Delta R_L \mathbf{g} \left(\frac{S}{L} \right) \\ a_g \approx \frac{1}{\lambda_F} \mathbf{g} \frac{1}{2\pi f \Delta C_L} \mathbf{g} \left(\frac{S}{L} \right) \end{array} \right. \quad (\text{S11})$$

$$\omega_f \approx \frac{2kL}{S \epsilon_{r1}} \quad (\text{S12})$$

$$\left\{ \begin{array}{l} a_g \approx \frac{\Delta R_L}{\omega_f} \mathbf{g} \mathbf{f} \\ a_g \approx \frac{1}{2\pi} \mathbf{g} \frac{1}{\omega_f} \mathbf{g} \frac{1}{\Delta C_L} \end{array} \right. \quad (\text{S13})$$

It is expressed as follows that the normalization of the output voltage and current:

$$\eta_V = \frac{V_L}{V_{oc}} \times 100\% \quad (\text{S14})$$

$$\eta_I = \frac{I_L}{I_{sc}} \times 100\% \quad (\text{S15})$$

Among them, the performance ratio of voltage and current, load voltage and current, as well as open-circuit voltage and short-circuit current are represented by η_V and η_I , V_L and V_{oc} , I_L and I_{sc} respectively.

Supplementary Note 2. Calculation of matching reactance of evaluation prototypes.

When the load reactance matches the internal reactance ($a_g=1$), the maximum power is produced by TENGs. According to the resistance calculation formula: $R = \rho T/S$, the internal resistances ($R_{\text{PTFE}}, R_{\text{Kapton}}$) of TENGs are displayed by Eqs. (S16), (S17) when the dielectric layer is PTFE and Kapton, respectively.

$$R_{\text{PTFE}} \approx \frac{10^{15} \times 10^{-10}}{10^{-3}} \approx 10^8 \ \Omega \quad (\text{S16})$$

$$R_{\text{Kapton}} \approx \frac{10^{14:15} \times 10^{-10}}{10^{-3}} \approx 10^{7:8} \ \Omega \quad (\text{S17})$$

where ρ, S stands for the resistivity of the dielectric layer and relative contact area of TENG. Moreover, the surface of the dielectric layer is polarized after TENG is electrified by friction, so T is the thickness of the triboelectric monolayer, which is generally about 10^{-10} m. Therefore, the internal resistance of C-S and S-E modes is $R_{\text{Kapton}} \approx 10^7 \sim 8 \ \Omega$, and that of L-S and F-S modes is $R_{\text{PTFE}} \approx 10^8 \ \Omega$.

Accord formula: $C = \epsilon_r \epsilon_0 S / 4\pi k d$, the internal constant capacitance ($C_{\text{P-1}}, C_{\text{K-1}}$) and variable capacitance ($C_{\text{P-0}}, C_{\text{K-0}}$) of TENGs are expressed as Eqs. (S18-21) when the dielectric layer is PTFE and Kapton, respectively.

$$C_{\text{P-1}} \approx \frac{10^{-11} \times 10^{-3}}{10^{-5}} \approx 10^{-10 \sim -9} \ \text{F} \quad (\text{S18})$$

$$C_{\text{K-1}} \approx \frac{10^{-11} \times 10^{-3}}{10^{-5}} \approx 10^{-9} \ \text{F} \quad (\text{S19})$$

$$C_{\text{P-0}} \approx \frac{10^{-11} \times 10^{-3}}{10^{-6 \sim -5}} \approx 10^{-9 \sim -8} \ \text{F} \quad (\text{S20})$$

$$C_{\text{K-0}} \approx \frac{10^{-11} \times 10^{-3}}{10^{-6 \sim -5}} \approx 10^{-9 \sim -8} \ \text{F} \quad (\text{S21})$$

where $\epsilon_r, \epsilon_0, d$ and S is relative dielectric constant, the vacuum dielectric constant, distance between two parallel plates of capacitance and the relative area.

For S-E and F-S modes, the inductive capacitances ($C_{\text{SE-0}}, C_{\text{FS-0}}$) are also generated in the substrate and dielectric layer.

$$C_{\text{SE-0}} \approx \frac{10^{-11} \times 10^{-3}}{10^{-5 \sim -4}} \approx 10^{-10 \sim -9} \ \text{F} \quad (\text{S22})$$

$$C_{FS-0} \approx \frac{10^{-11} \times 10^{-3}}{10^{-4 \sim -5}} \approx 10^{-10 \sim -9} \text{ F} \quad (\text{S23})$$

Because the capacitances are in series, the total capacitance is smaller than the smallest capacitance. Additionally, Table S3 displays the specific internal resistance and capacitance. The capacitances of C-S (C_{CS}), L-S (C_{LS}), S-E (C_{SE}) and F-S (C_{FS}) modes TENGs are the inherent capacitance ($C_{CS} \approx 10^{-9} \text{ F}$, $C_{LS} \approx 10^{-10 \sim -9} \text{ F}$) and inductive capacitance ($C_{SE} \approx 10^{-10 \sim -9} \text{ F}$, $C_{FS} \approx 10^{-10 \sim -9} \text{ F}$), respectively. Overall, the above formula is only an empirical formula, and it can be used to quickly determine internal resistance and capacitance.